—Original—

The Contribution of Alcohol Dehydrogenase 3 to the Development of Alcoholic Osteoporosis in Mice

Takahisa Okuda[1]*, Munehiro Naruo[1], Osamu Iijima[2], Tsutomu Igarashi[3], Midori Katsuyama[1], Motoyo Maruyama[4], Toshio Akimoto[4], Youkichi Ohno[1] and Takeshi Haseba[1,5]*

[1]Department of Legal Medicine, Nippon Medical School, Tokyo, Japan
[2]Office for Research Administrative Support, Center for Strategic Research Initiative, Nippon Medical School, Tokyo, Japan
[3]Department of Ophthalmology, Nippon Medical School, Tokyo, Japan
[4]Division of Laboratory Animal Science, Nippon Medical School, Tokyo, Japan
[5]Department of Legal Medicine, Kanagawa Dental University, Kanagawa, Japan

Background: Alcohol dehydrogenase 3 (ADH3) plays major roles not only in alcohol metabolism but also in nitric oxide metabolism as S-nitrosoglutathione reductase (GSNOR). ADH3/GSNOR regulates both adipogenesis and osteogenesis through the denitrosylation of peroxisome proliferator-activated receptor γ. The current study investigated the contribution of ADH3 to the development of alcoholic osteoporosis in chronic alcohol consumption (CAC).

Methods: Nine-week-old male mice of different ADH genotypes [wild-type (WT) and *Adh3*$^{-/-}$] were administered a 10% ethanol solution for 12 months. The femurs were evaluated by histochemical staining and computed tomography-based bone densitometry. The mRNA levels of ADH3 were evaluated in the WT mice by reverse transcription-quantitative polymerase chain reaction.

Results: The *Adh3*$^{-/-}$ control mice exhibited increased activities of both osteoblasts and osteoclasts and lower bone masses than the WT control mice. CAC exhibited no remarkable change in osteoblastic and osteoclastic activities, but decreased bone masses were observed in WT mice despite an increase in the mRNA levels of ADH3. Conversely, bone masses in the *Adh3*$^{-/-}$ control mice were not reduced after CAC.

Conclusions: The *Adh3*$^{-/-}$ control mice exhibited a high turnover of osteoporosis since osteoclastogenesis dominated osteoblastogenesis; however, bone resorption was not enhanced after CAC. In comparison, CAC lead to alcoholic osteoporosis in WT mice, accompanied by increased mRNA levels of ADH3. Hence, ADH3 can prevent osteoporosis development in normal ADH genotypes with no alcohol ingestion. However, ADH3 contributes to the development of alcoholic osteoporosis under CAC by participating in alcohol metabolism, increasing metabolic toxicity, and lowering GSNO reducing activity.

(J Nippon Med Sch 2018; 85: 322–329)

Key words: ADH3, GSNOR, alcoholic osteoporosis, chronic alcohol consumption, osteoclastogenesis

Introduction

Alcohol dehydrogenase (ADH; EC 1.1.1.1) catalyzes the oxidation of alcohol to acetaldehyde in alcohol metabolism. ADH3 (x-ADH, Class III ADH, or *Adh5*) is a member of ADH family that was initially reported by Haseba et al (1979)[1] and Parés[2]. It is highly conserved from bacteria to humans and ubiquitously distributed in mammalian tissues[3]. Several unique functions have been recognized, such as alcohol metabolism, detoxification of formaldehyde, and S-nitrosoglutathione (GSNO) reducing

*T. Okuda and T. Haseba contributed equally to this study.

Correspondence to Takahisa Okuda, MD, PhD, Department of Legal Medicine, Nippon Medical School, 1–1–5 Sendagi, Bunkyo-ku, Tokyo 113–8602, Japan
E-mail: ta-okuda@nms.ac.jp
Journal Website (http://www2.nms.ac.jp/jnms/)

activity[4]. With regard to alcohol metabolism, the activity of ADH3 towards ethanol is usually low due to its high K_m; however, we reported an *in vitro* study showing that the hydrophobicity of the solution markedly lowered the K_m of ADH3 to increase the catalytic efficiency (K_{cat}/K_m)[5,6]. In addition, we reported that pyrazole insensitive-ADH, which was identical to ADH3, played a significant role in alcohol metabolism in cases of alcoholic patients with liver disease[7]. We have recently reported that ADH3 dose-dependently participated in systemic alcohol metabolism[6] and ADH3 liver content was significantly correlated with the rate of alcohol metabolism[8]. Furthermore, a recent study suggested that acetaldehyde generated by ADH3 in the hippocampus participated in the synaptic dysfunction in acute alcohol intoxication resulting in the development of alcohol-induced blackouts[9]. These studies revealed that the ADH3-mediated oxidative pathway of ethanol is an additional pathway, instead of the classical pathway mediated by ADH1 at high blood alcohol concentrations such as binge alcohol-drinking or chronic alcohol consumption (CAC).

In addition to alcohol metabolism, ADH3 serves an important regulatory function in nitric oxide (NO) signaling through the GSNO reducing activity[10] and is referred to as GSNO reductase (GSNOR)[4]. ADH3 regulates S-nitrosylation of proteins by the degradation of GSNO, resulting in decreasing S-nitrosylated proteins[4,11]. A recent study suggested that the peroxisome proliferator-activated receptor γ (PPARγ), a key regulator of both adipogenesis and osteogenesis, is controlled by NO through S-nitrosylation. According to the study, the *GSNOR*-null mutant mice which were identical to the *Adh3*-null mutant mice exhibited decreased fat mass and increased bone formation accompanied by increased bone resorption[11].

Alcohol consumption affects bone metabolism, bone mass, and bone strength. Light alcohol consumption provides several beneficial effects to bone[12,13], whereas heavy CAC is detrimental to bone and is known to induce secondary osteoporosis[13,14]. The decrease in bone mass and strength following CAC might be due to bone remodeling imbalance with a predominant decrease in bone formation[14,15]. Although ADH3 plays a major role in alcohol metabolism and osteogenesis, detailed studies focusing on the effect of ADH3 on bone formation during CAC are lacking. In this study, chronic ethanol administration to mice with different ADH genotypes [C57BL/6N as wild-type (WT) and *Adh3*-null mutant mice] was carried out for 12 months in order to investigate the contribution of ADH3/GSNOR to the development of alcoholic osteoporosis.

Materials and Methods

Mice

Mice carrying the homozygous null mutant of the ADH3 gene ($Adh3^{-/-}$) were used in this study. The original knockout mice obtained from the Burnham Institute (La Jolla, CA, USA) in 1999[16] were backcrossed with a background strain of C57BL/6 wild-type mice (Sankyo Lab Co., Ltd., Tokyo, Japan) for up to 13 generations. The congenic strains of $Adh3^{-/-}$ mice have been maintained in Nippon Medical School (Tokyo, Japan) since 2013. The WT and $Adh3^{-/-}$ mice were selectively housed (5–8 mice/cage) in a polycarbonate cage bedded with white flakes at 24±2℃ with a 14 h light/10 h dark cycle beginning at 7:00 a.m. The animals were fed commercial rodent food (MF pellets, Oriental Yeast Co., Ltd., Tokyo, Japan) *ad libitum* in a specific pathogen-free facility. All animal experiments were conducted in compliance with the protocol reviewed by the Institutional Committee of Laboratory Animals and approved by the President of the Nippon Medical School (approval number 28-001). The protocol was based on "The Guidelines of the International Committee on Laboratory Animals 1974."

Ethanol Administration to Mice

Nine-week-old male mice in the different ADH genotypes were randomly assigned to the ethanol group [WT (E) or $Adh3^{-/-}$ (E); n=5 each] and the control group [WT (C) or $Adh3^{-/-}$ (C); n=5 each]. The ethanol group was administered 10% (w/v) ethanol/water solution *ad libitum* for 12 months as the sole drinking fluid for the CAC experiment. The concentration of the ethanol solution was increased in a gradient up to 10% until the week before the start of the experiment. The mice in the control group were provided with only water to drink for 12 months. Integral ethanol consumption was calculated from the amount of daily ethanol consumption and expressed as grams of the ethanol/gram of the mouse's body weight.

Histochemical Tartrate-resistant Acid Phosphatase and Alkaline Phosphatase Activity Staining

After CAC for 12 months, the mice were anesthetized with an intraperitoneal injection of a combination anesthetic (0.3 mg/kg of medetomidine, 4.0 mg/kg of midazolam, and 5.0 mg/kg of butorphanol), followed by cervical dislocation. The bilateral femurs were harvested, cleaned from soft tissues, rinsed with cold saline, and measured. Histochemical tartrate-resistant acid phosphatase (TRAP) and alkaline phosphatase (ALP) activity

Table 1 Reverse-transcriptase-quantitative polymerase chain reaction sequence of primers

Access ion no.	Gene name (genetic symbol)	Forward primer	Reverse primer
NM_007 393.5	Mus musculus actin, beta (*Actb*), mRNA	GCGCAAGTTAGGTTTTGTCAAAG	TGGATCAGCAAGCAGGAGTAC
NM_007 410.3	Mus musculus alcohol dehydrogenase 5 (class III), chi polypeptide (*Adh5*), transcript variant 1, mRNA	ACAGGAAAGAGTGCAGGATGG	TTGTGACCGGCAATCTCTCC

The gene encoding the mammalian ADH3 has been termed *Adh5*.

staining was performed using a previously described method[17]. Briefly, the femur was fixed with 4% paraformaldehyde for two days, followed by fixation with 30% sucrose for a week without decalcification. It was then embedded in the optimum cutting temperature (O.C.T.) compound (Sakura Finetek Japan Co Ltd., Tokyo, Japan) and stored at −80℃. Frozen sections (7 μm thick) were cut using the Kawamoto film method[18], and histochemical TRAP/ALP activity was assayed according to the manufacturer's protocol (Wako Pure Chemical Industries Ltd., Osaka, Japan). Photographic images were taken with a light microscope (BX 60; Olympus Ltd., Tokyo, Japan) at 20X magnification and cellSens standard software version 1.4.1 (Olympus Ltd.) was used to manually stitch the images.

Bone Morphometrical Analyses by Quantitative CT

Bone morphometrical analyses were performed using a Latheta experimental animal computed tomography (CT) system (LCT-200; Hitachi Healthcare BU, Tokyo, Japan). Briefly, the left femur was fixed in 70% ethanol for 1 week. CT scans were performed with a voxel size of 24× 48 μm at a tube voltage of 50 kVp, a tube current of 0.5 mA, an integration time of 26 ms for each projection, and an axial field view of 200 mm. The bone morphometry was evaluated according to the standard method provided by Bouxsein *et al*.[19]. In order to evaluate the trabecular bone morphometry, the bone morphometrical parameters, including trabecular bone volume (trabecular BV; cm^3), total volume (TV; cm^3) and bone volume fraction (BV/TV; %), were assayed directly above the growth plate in the distal femur. In order to evaluate the cortical bone morphometry, cortical bone area (Ct.Ar; cm^2), total cross section area (Tt.Ar; cm^2), cortical bone fraction (Ct. Ar/Tt.Ar; %), and cortical thickness (Ct.Th; cm) were assayed in a central part of the femur diaphysis. Furthermore, the flexural rigidity (I_{min}; mg・cm), which represents the minimum moment of inertia of cross-sectional areas, and torsional rigidity (J; mg・cm), which represents the polar moment of inertia of cross-sectional areas, were also assayed in the central femur diaphysis. The bone morphometric parameters were calculated using Latheta software version 3.44 (Hitachi Healthcare BU).

Quantification of Alcohol Dehydrogenase 3 mRNA Using Reverse Transcription-quantitative Polymerase Chain Reaction

The mRNA levels of ADH3 in the condyle of the right femurs were determined by reverse transcription-quantitative polymerase chain reaction (RT-qPCR) analysis. Total RNA was extracted from the powdered condyle (30 mg) using a Qiagen RNeasy Mini Kit (QIAGEN, Hilden, Germany) by DNase digestion. Reverse transcription was performed using a High Capacity cDNA Reverse Transcription kit (Applied Biosystems, Foster City, CA, USA) according to the manufacturer's protocol, followed by RT-qPCR on an ABI 7500 Fast Real-Time PCR System (Applied Biosystems), as described previously[8,20]. The gene-specific primers were designed using Primer-3-Plus (http://primer3plus.com; **Table 1**). The data were analyzed by ABI 7500 Software version 2.3 (Applied Biosystems). The threshold cycle (Ct) values of the genes were normalized against that of β-*actin* using the $2^{-\Delta\Delta Ct}$ method.

Statistical Analysis

Results are expressed as means±SD. Statistical significance was assessed by the Student-Newman-Keuls method (ystat2013, Igaku-shoin, Tokyo, Japan) to determine the interaction of genotypes and ethanol effects. The level of significance was considered at $p<0.05$.

Results

Baseline Characteristics of Mice

The WT (E) mice were significantly heavier than the WT (C) mice ($p<0.05$), whereas the *Adh3*$^{-/-}$ mice exhibited no difference in the weights between the ethanol and control groups. No significant difference was observed in the length of femurs between the two groups of the WT and *Adh3*$^{-/-}$ mice. Integral ethanol consumption was found to be higher in the *Adh3*$^{-/-}$ (E) mice than the WT

(E) mice throughout the study. The WT (E) and *Adh3*$^{-/-}$ (E) mice achieved 3.269 g of ethanol/g of body weight and 4.168 g of ethanol/g of body weight, respectively, at the end of the experimental period.

Histochemical Views of Tartrate-resistant Acid Phosphatase and Alkaline Phosphatase Activity Staining

The histochemical views of TRAP/ALP activity staining are shown in **Figure 1**. The osteoclastic activities by TRAP staining and the osteoblastic activities by ALP staining were observed along the endosteal bone surfaces. When the ADH genotypes in the control group were compared, the *Adh3*$^{-/-}$ (C) bone exhibited higher activities of both osteoclasts and osteoblasts than the WT (C) bone. CAC exhibited no remarkable change in osteoblastic and osteoclastic activities in WT mice. Conversely, both osteoclastic and osteoblastic activities were decreased in the *Adh3*$^{-/-}$ bones by CAC.

Trabecular Bone Morphometry Above the Growth Plate

The results of trabecular BV, TV, and trabecular BV/TV above the growth plate are shown in **Figure 2**. Upon comparison between the ADH genotypes in the control group, it was observed that the trabecular BV and trabecular BV/TV were significantly higher in the WT mice than the *Adh3*$^{-/-}$ mice (**Fig. 2A, 2C**), whereas no significant difference was noted in the TV (**Fig. 2B**). Similar changes were observed in the WT (C) mice compared to the WT (E) mice (**Fig. 2A-C**). No significant difference was observed in the *Adh3*$^{-/-}$ mice after CAC in the trabecular bone. The representative axial images right above the growth plate in each group are shown in **Figure 2D**.

Cortical Bone Morphometry in the Middle of the Femur Diaphysis

The results of Ct.Ar, Tt.Ar, Ct.Ar/Tt.Ar, Ct.Th, I_{min}, and *J* at the central part of the femur diaphysis are shown in **Figure 3**. The Ct.Ar and Tt.Ar were significantly higher in the WT (C) mice than the *Adh3*$^{-/-}$ (C) mice (**Fig. 3A, 3B**), whereas no significant difference was observed in the Ct.Ar/Tt.Ar and Ct.Th (**Fig. 3C, 3D**). The I_{min}, and *J* were significantly higher in the WT (C) mice than the *Adh3*$^{-/-}$ (C) mice (**Fig. 3E, 3F**). The Tt.Ar, Ct.Ar, Ct.Th, and rigidities were decreased significantly in the WT mice after CAC (**Fig. 3A-F**). No significant difference was observed in the *Adh3*$^{-/-}$ mice after CAC in the cortical bone at the central femur diaphysis (**Fig. 3A-F**).

Quantification of Alcohol Dehydrogenase 3 mRNA

The mRNA levels of ADH3 in the condyle were significantly higher in the WT (E) than the WT (C) mice (**Fig. 4**).

Discussion

Alcohol dehydrogenases are a part of the oxidoreductase family. ADH3 is considered to be the ancestral enzyme among members of the ADH family[3,4]. It is distributed in almost all the tissues in mammals and strongly involved in the essential cellular pathways[3,4]. ADH3 plays major roles not only in alcohol metabolism but also in nitric oxide (NO) metabolism as GSNOR[3,4]. ADH3/GSNOR regulates both adipogenesis and osteogenesis through the GSNOR-mediated PPARγ denitrosylation[11]. The extent of PPARγ nitrosylation is governed by the equilibrium between nitrosylation and denitrosylation reactions[11]. Therefore, the role of ADH3/GSNOR in bone metabolism is to maintain the equilibrium between PPARγ and S-nitrosylated PPARγ, regulating differentiation of MSCs into osteoblasts.

In the current study, we performed the histochemical TRAP/ALP activity staining to the femur of mice with different ADH genotypes. The results indicated that osteoblastic activity increased in the *Adh3*$^{-/-}$ (C) mice when compared to the WT (C) mice, accompanied by an increase in osteoclastic activity, which was consistent with the results of the previous *in vitro* study[11]. Furthermore, the bone morphometrical CT analyses revealed that the bone mass and the bone strength were significantly lower in the *Adh3*$^{-/-}$ (C) mice than the WT (C) mice. These findings suggested that ADH3 promoted not only osteoblastogenesis but also osteoclastogenesis, thus providing a new insight into the role of ADH3. The *Adh3*$^{-/-}$ (C) mice were expected to demonstrate an increase of S-nitrosylated PPARγ due to the lack of GSNO reducing activity. It has been proven that excessive S-nitrosylated PPARγ contributes to diminished adipogenic and increased osteoblastic differentiation[11]. In addition, it has been reported that PPARγ and its ligand promote osteoclast differentiation by directly regulating c-Fos expression in the nuclear factor-κB ligand (RANKL) signaling pathway[21]. Nakanishi *et al.*[22] also demonstrated that osteoclastogenesis was activated by PPARγ-mediated enhancement of c-Fos expression. These findings suggested that the increased osteoclastic activities in the *Adh3*$^{-/-}$ (C) mice could be attributed to the enhanced c-Fos expression by the accumulation of S-nitrosylated PPARγ due to the lack of ADH3. The imbalance between the bone formation by osteoblasts and bone resorption by osteoclasts resulted in exhibiting high-turnover osteoporosis in bone metabolism in the *Adh3*$^{-/-}$ (C) mice.

Alcoholic osteoporosis is well recognized as one of the common alcohol-use disorders[23]. Numerous studies have

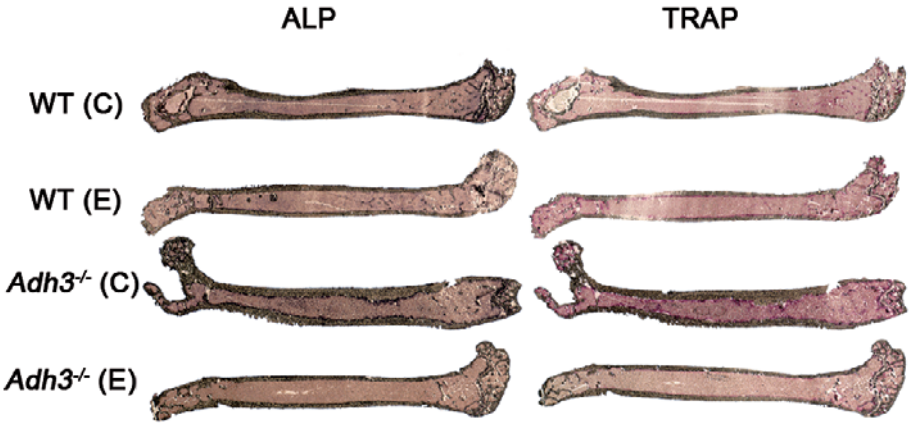

Fig. 1 Histochemical images of TRAP/ALP activity staining. The activities of osteoblasts and osteoclasts were evaluated by TRAP/ALP activity staining. The photographic images were taken at 20X magnification and manually stitched together. The gray scale bars represent 2 mm. TRAP, tartrate-resistant acid phosphatase; ALP, alkaline phosphatase; *Adh*, alcohol dehydrogenase; WT, wild-type mouse (*C57BL/6N*); *Adh3*$^{-/-}$, *ADH3* knockout mouse; (C), the mice were provided water in the control group; (E), the mice were administered ethanol in the ethanol group.

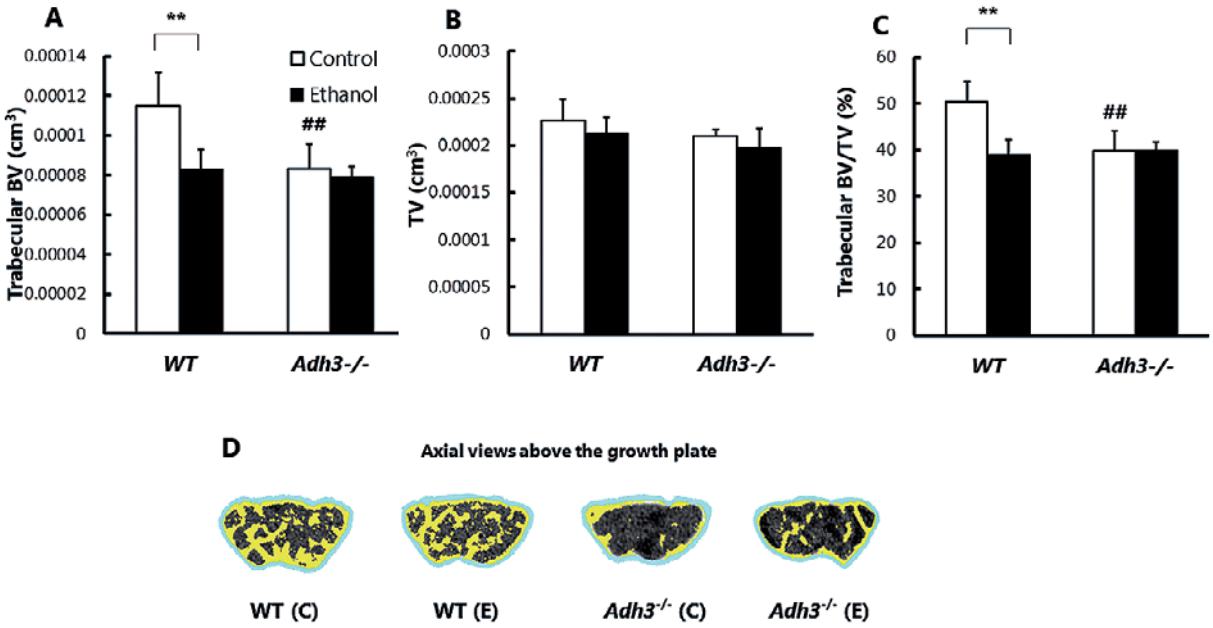

Fig. 2 CT-based bone densitometry at the proximal portion of the growth plate. Trabecular BV (A), TV (B), and trabecular BV/TV (C) above the growth plate. The *white bars* represent the mice that were provided water (control groups), and the *black bars* represent the mice that were administered a 10% ethanol (w/v) solution for 12 months (ethanol groups). $^{**}p<0.01$ between the control and ethanol group as assayed by the Student-Newman-Keuls method. $^{\#\#}p<0.01$ between the WT control mice and *Adh3*$^{-/-}$ control mice as assayed by the Student-Newman-Keuls method. (D) The representative axial images above the growth plate in each group. Yellow areas represent trabecular bone, and blue areas represent cortical bone. BV, bone volume; TV, total volume; *Adh*, alcohol dehydrogenase; WT, wild-type mouse (*C57BL/6N*); *Adh3*$^{-/-}$, *ADH3* knockout mouse. (C), the mice were provided with water in the control group; (E), the mice were administered ethanol in the ethanol group.

reported that CAC lowers bone mineral content and bone mineral density and disrupts trabecular microarchitecture[13–15]. The effect of CAC on bone can be both direct and indirect[24]; direct toxic effects resulted in the inhibition of osteoblast proliferation and function *in vitro*[25] and an increase in the number of osteoclasts[26]. Indirect effects are mainly linked to impaired nutrition and hormone alteration, which may change the activities of osteoblasts and osteoclasts[24]. Another consequence is tissue damage caused by secondary metabolites such as acetaldehyde.

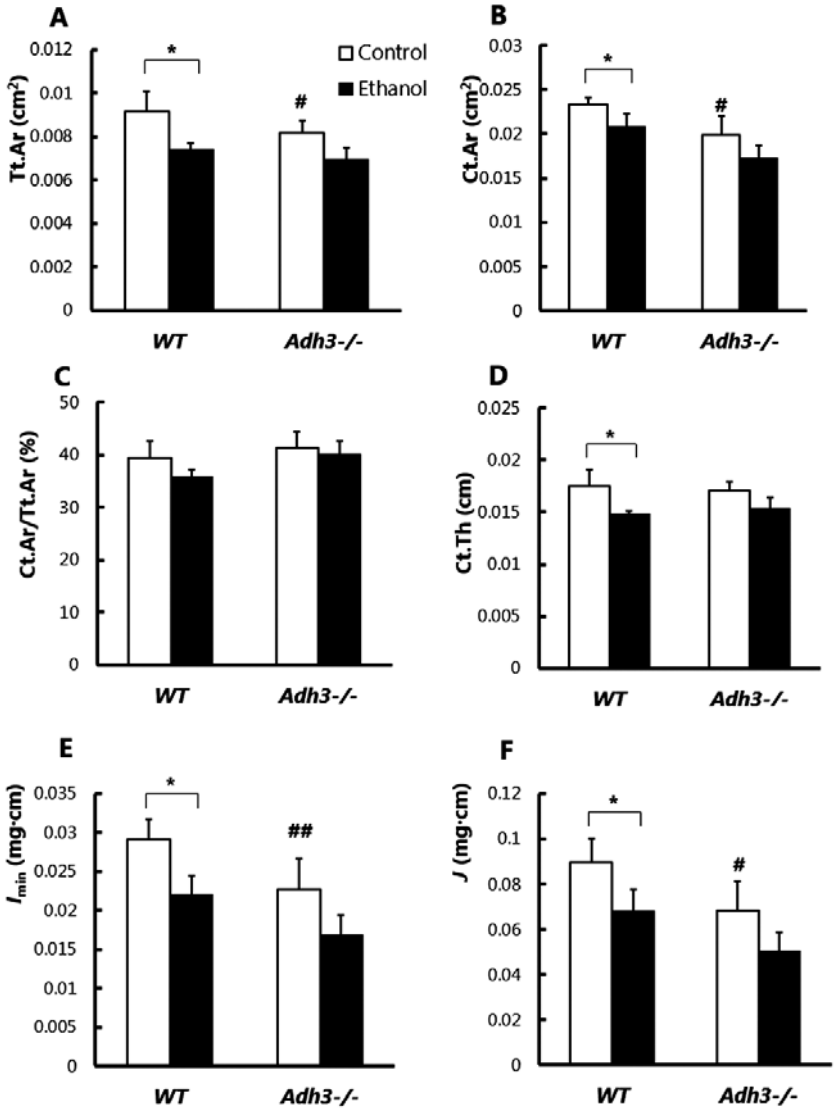

Fig. 3 CT-based bone densitometry and rigidity in the middle of the femur diaphysis. Ct.Ar (A), Tt.Ar (B), Ct.Ar/Tt.Ar (C), Ct.Th (D), I_{min} (E), and J (F) at the central part of the femur diaphysis. The *white bars* represent the mice that were provided with water (control groups), and the *black bars* represent the mice that were administered 10% ethanol (w/v) solution for 12 months (ethanol groups). *p<0.05 between the control and ethanol group as assayed by the Student-Newman-Keuls method. #p<0.05 and ##p<0.01 between the WT control mice and *Adh3*$^{-/-}$ control mice as assayed by the Student-Newman-Keuls method. Ct.Ar, cortical bone area; Tt.Ar, total cross section area; Ct.Ar/Tt.Ar, cortical bone fraction; Ct.Th, cortical thickness; I_{min}, flexural rigidity; J, torsional rigidity; *Adh*, alcohol dehydrogenase; WT, wild-type mouse (*C57BL/6N*); *Adh3*$^{-/-}$, *ADH3* knockout mouse.

Several studies reported that acetaldehyde inhibited osteoblastic proliferation and activities[27,28] and induced osteoclastic activities by increasing RANKL mRNA expression[29]. In the current study, the histochemical TRAP/ALP staining revealed that osteoblastic and osteoclastic activity showed no remarkable changes in WT mice after CAC; however, comparison of the CT-based bone densitometry in the WT (E) and (C) mice showed that bone mass or bone rigidity was decreased in both trabecular and cortical bones, indicating that alcoholic osteoporosis progressed in the current experimental condition. Díez *et al.*[30] reported that chronic alcohol abusers in the absence of severe chronic liver damage exhibited a significant decrease in BV and BV/TV, accompanied by an increase in osteoclast number. In comparison, the 14-month-old mice used in our experiment seemed to be too old to show an

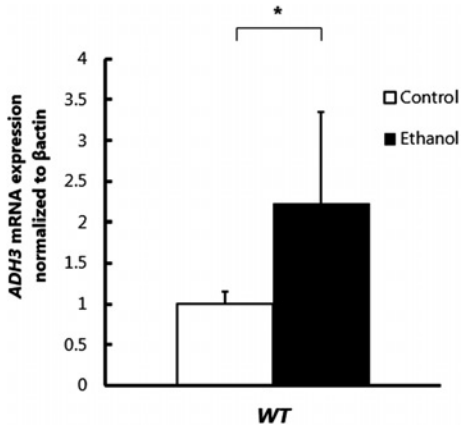

Fig. 4 The mRNA level of ADH3. The *white bar* represents the mice that were given water (control groups), and the *black bar* represents the mice that were given a 10% ethanol w/v solution (ethanol groups). *$p<0.05$ between the control and ethanol groups in the WT mice by the Student-Newman-Keuls method. ADH, alcohol dehydrogenase; *Adh3*$^{-/-}$, *ADH3* knockout mouse.

increase in osteoclastic activity. Hence, osteoclastogenesis dominated osteoblastogenesis in WT mice after CAC despite the results of histochemical TRAP/ALP staining. Conversely, the histochemical TRAP/ALP activity staining in the *Adh3*$^{-/-}$ mice revealed that the activities of both osteoclasts and osteoblasts were reduced after CAC. Although the *Adh3*$^{-/-}$ mice consumed much more alcohol than the WT mice, the bone masses, which were already low in the *Adh3*$^{-/-}$ control mice, were not significantly reduced, indicating that bone resorption was not enhanced after CAC.

The mRNA analyses in the WT mice exhibited increased mRNA levels of ADH3 after CAC, although alcoholic osteoporosis progressed. The results seemed to be contradictory since the *Adh3*$^{-/-}$ (C) mice exhibited increased osteoclastic activity due to the lack of GSNO reducing activity. It has been hypothesized that the mRNA levels of ADH3 might be increased due to metabolic adaptation to CAC[8]. The increased ADH3 in the bone might participate in the local metabolism of ethanol and generate secondary metabolites, which may cause the bone tissue damage in WT mice. In addition, the primary physiological role of ADH3 as GSNOR in bone metabolism may be inhibited by CAC due to the participation in alcohol metabolism. Similar inhibition is recognized when ethanol inhibits Vitamin A metabolism through ADH in the testes and possibly induces sterility[31].

The current results suggest that the *Adh3*$^{-/-}$ control mice exhibited a high turnover of osteoporosis since osteoclastogenesis dominated osteoblastogenesis; however, bone resorption was not enhanced after CAC. In comparison, CAC lead to alcoholic osteoporosis in WT mice, accompanied by increased mRNA levels of ADH3. Hence, ADH3 can prevent osteoporosis development in normal ADH genotypes with no alcohol ingestion. However, ADH3 contributes to the development of alcoholic osteoporosis under CAC by participating in alcohol metabolism, increasing metabolic toxicity, and lowering GSNO reducing activity.

Acknowledgements: This study was supported by the Japan Society for the Promotion of Science (JSPS) KAKENHI Grant Number 16K09223.

Conflict of Interest: All authors declare no conflict of interest related to this study.

References

1. Haseba T, Hirakawa K, Nihira M, Hayashida M, Kurosu M, Tomita Y, Ide T, Watanabe T: Partial purification and characterization of alcohol dehydrogenases from mouse liver. J Stud Alcohol 1979; 14: 324. (in Japanese).
2. Parés X, Vallee BL: New human liver alcohol dehydrogenase forms with unique kinetic characteristics. Biochem Biophys Res Commun 1981; 98: 122–130.
3. Liu L, Hausladen A, Zeng M, Que L, Heitman J, Stamler JS: A metabolic enzyme for S-nitrosothiol conserved from bacteria to humans. Nature 2001; 410: 490–494.
4. Haseba T, Ohno Y: A new view of alcohol metabolism and alcoholism--role of the high-Km Class III alcohol dehydrogenase (ADH3). Int J Environ Res Public Health 2010; 7: 1076–1092.
5. Yamamoto I, Haseba T, Kurosu M, Watanabe T: Allosterism of acidic alcohol dehydrogenase (Class III ADH) of mouse liver and its role in alcohol metabolism. J Nippon Med Sch 1992; 59: 38–46. (in Japanese).
6. Haseba T, Duester G, Shimizu A, Yamamoto I, Kameyama K, Ohno Y: In vivo contribution of Class III alcohol dehydrogenase (ADH3) to alcohol metabolism through activation by cytoplasmic solution hydrophobicity. Biochim Biophys Acta 2006; 1762: 276–283.
7. Kamii H: Pyrazole sensitive and pyrazole insensitive-alcohol dehydrogenase activities in biopsied livers of patients with alcoholic liver disease. J Nippon Med Sch 1988; 55: 236–246. (in Japanese).
8. Okuda T, Haseba T, Katsuyama M, Maruyama M, Akimoto T, Igarashi T, Ohno Y: Metabolic pharmacokinetics of early chronic alcohol consumption mediated by liver alcohol dehydrogenases 1 and 3 in Mice. J Gastroenterol Hepatol 2018. (epub ahead of print).
9. Tokuda K, Izumi Y, Zorumski CF: Locally-generated Acetaldehyde Contributes to the Effects of Ethanol on Neurosteroids and LTP in the Hippocampus. Neurol Clin Neurosci 2013; 1: 138–147.
10. Hess DT, Matsumoto A, Kim SO, Marshall HE, Stamler JS: Protein S-nitrosylation: purview and parameters. Nat Rev Mol Cell Biol 2005; 6: 150–166.
11. Cao Y, Gomes SA, Rangel EB, Paulino EC, Fonseca TL, Li

J, Teixeira MB, Gouveia CH, Bianco AC, Kapiloff MS, Balkan W, Harel JM: S-nitrosoglutathione reductase-dependent PPARγ denitrosylation participates in MSC-derived adipogenesis and osteogenesis. J Clin Invest 2015; 125: 1679–1691.
12. Feskanich D, Korrick SA, Greenspan SL, Rosen HN, Colditz GA: Moderate alcohol consumption and bone density among postmenopausal women. J Womens Health 1999; 8: 65–73.
13. Jang HD, Hong JY, Han K, Lee JC, Shin BJ, Choi SW, Suh SW, Yang JH, Park SY, Bang C: Relationship between bone mineral density and alcohol intake: A nationwide health survey analysis of postmenopausal women. PLoS One 2017; 12: e0180132.
14. Laitinen K, Lamberg-Allardt C, Tunninen R, Härkönen M, Välimäki M: Bone mineral density and abstention-induced changes in bone and mineral metabolism in non-cirrhotic male alcoholics. Am J Med 1992; 93: 642–650.
15. Diamond T, Stiel D, Lunzer M, Wilkinson M, Posen S: Ethanol reduces bone formation and may cause osteoporosis. Am J Med 1989; 86: 282–288.
16. Duester G, Farrés J, Felder MR, Holmes RS, Höög JO, Parés X, Plapp BV, Yin SJ, Jörnvall H: Recommended nomenclature for the vertebrate alcohol dehydrogenase gene family. Biochem Pharmacol 1999; 58: 389–395.
17. Iijima O, Miyake K, Watanabe A, Miyake N, Igarashi T, Kanokoda C, Nakamura-Takahashi A, Kinoshita H, Noguchi T, Abe S, Narisawa S, Millán JL, Okada T, Shimada T: Prevention of Lethal Murine Hypophosphatasia by Neonatal Ex Vivo Gene Therapy Using Lentivirally Transduced Bone Marrow Cells. Hum Gene Ther 2015; 26: 801–812.
18. Kawamoto T: Use of a new adhesive film for the preparation of multi-purpose fresh-frozen sections from hard tissues, whole-animals, insects and plants. Arch Histol Cytol 2003; 66: 123–143.
19. Bouxsein ML, Boyd SK, Christiansen BA, Guldberg RE, Jepsen KJ, Müller R: Guidelines for assessment of bone microstructure in rodents using micro-computed tomography. J Bone Miner Res 2010; 25: 1468–1486.
20. Katsuyama M, Demura M, Katsuyama H, Tanii H, Saijoh K: Genistein and menaquinone-4 treatment-induced alterations in the expression of mRNAs and their products are beneficial to osteoblastic MC3T3-E1 cell functions. Mol Med Rep 2017; 16: 873–880.
21. Wan Y, Chong LW, Evans RM: PPAR-gamma regulates osteoclastogenesis in mice. Nat Med 2007; 13: 1496–1503.
22. Nakanishi A, Tsukamoto I: n-3 polyunsaturated fatty acids stimulate osteoclastogenesis through PPARγ-mediated enhancement of c-Fos expression, and suppress osteoclastogenesis through PPARγ-dependent inhibition of NFkB activation. J Nutr Biochem 2015; 26: 1317–1327.
23. Schuckit MA: Alcohol-use disorders. Lancet 2009; 373: 492–501.
24. Maurel DB, Boisseau N, Benhamou CL, Jaffre C: Alcohol and bone: review of dose effects and mechanisms. Osteoporos Int 2012; 23: 1–16.
25. Sun T, Deng Z, Zhu Y: Effects of insulin-like growth factor 1 on inhibition of osteoblastic proliferation and function by ethanol. Zhongguo Xiu Fu Chong Jian Wai Ke Za Zhi 2007; 21: 1338–1341.
26. Cheung RC, Gray C, Boyde A, Jones SJ: Effects of ethanol on bone cells in vitro resulting in increased resorption. Bone 1995; 16: 143–147.
27. Hurley MM, Martin DL, Kream BE, Raisz LG: Effects of ethanol and acetaldehyde on collagen synthesis, prostaglandin release and resorption of fetal rat bone in organ culture. Bone 1990; 11: 47–51.
28. Giuliani N, Girasole G, Vescovi PP, Passeri G, Pedrazzoni M: Ethanol and acetaldehyde inhibit the formation of early osteoblast progenitors in murine and human bone marrow cultures. Alcohol Clin Exp Res 1999; 23: 381–385.
29. Chen JR, Haley RL, Hidestrand M, Shankar K, Liu X, Lumpkin CK, Simpson PM, Badger TM, Ronis MJ: Estradiol protects against ethanol-induced bone loss by inhibiting up-regulation of receptor activator of nuclear factor-kappaB ligand in osteoblasts. J Pharmacol Exp Ther 2006; 319: 1182–1190.
30. Díez A, Puig J, Serrano S, Mariñoso ML, Bosch J, Marrugat J, Mellibovsky L, Nogués X, Knobel H, Aubía J: Alcohol-induced bone disease in the absence of severe chronic liver damage. J Bone Miner Res 1994; 9: 825–831.
31. Van Thiel DH, Gavaler J, Lester R: Ethanol inhibition of vitamin A metabolism in the testes: possible mechanism for sterility in alcoholics. Science 1974; 186: 941–942.

(Received, July 17, 2018)
(Accepted, October 2, 2018)